

This version of the ESI published 02/12/2025 replaces the previous version published 12/11/2025.

Regulating the photoelectric properties of porphyrin-based COF nanozymes by pillararene with polyphenol structure for efficient photo-enhanced antibacterial effect

Yahui Liu,^{a†} Jia Wen,^{*b†} Bingqian Ge,^a Tingting Guo,^a Jiaqi Li,^a Lingshan Jia,^a shoupeng Cao,^c Wei Li^{*a} and Kui Yang^{*a}

^a State Key Laboratory of New Pharmaceutical Preparations and Excipients, Key Laboratory of Medicinal Chemistry and Molecular Diagnosis of the Ministry of Education, College of Chemistry and Materials Science, Hebei University, Baoding 071002, P. R. China, E-mail: yangkuihbu@126.com (K. Yang); liweihebeilab@163.com (W. Li).

^b College of Pharmaceutical Science, Hebei University, Baoding 071002, P. R. China, E-mail: wenjiahbu@163.com (J. Wen).

^c State Key Laboratory of Polymer Materials Engineering, College of Polymer Science and Engineering, Sichuan University, Chengdu 610065, P. R. China.

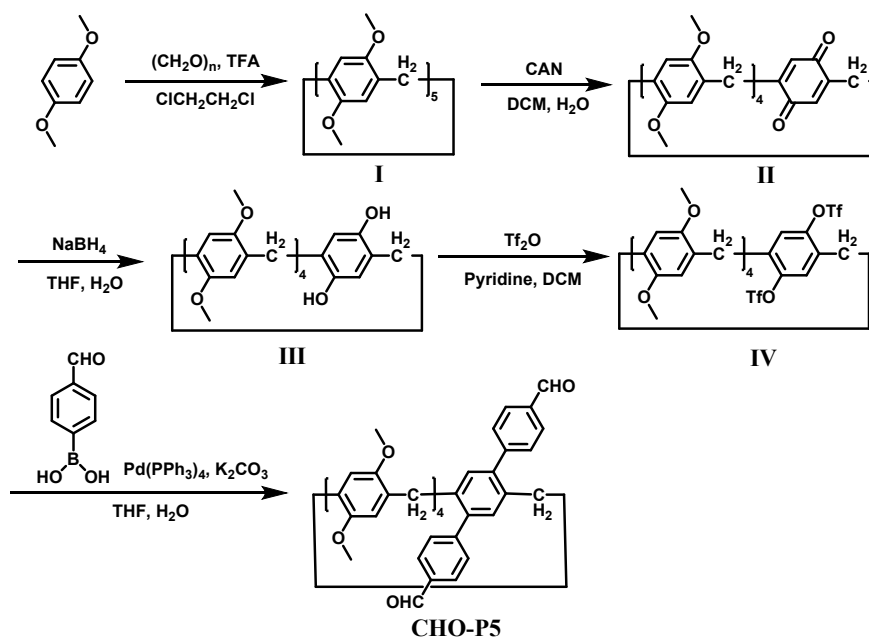
† These authors contribute equally to this work.

1. Materials and instruments

All solvents and chemical reagents were purchased from commercial reagents corporation and used without further purification. The compositions of synthesized materials were characterized by nuclear magnetic resonance (NMR; BUXI-INMR, Wuhan). The morphologies and compositions of the materials were characterized by scanning electron microscope (SEM; Nova NanoSEM450, USA), transmission electron microscopy (TEM; JEM2100PLUS, Japan), atomic force microscopy (AFM; Bruker Dimension Icon, Germany), thermogravimetric analysis (TGA; NETZSCH STA 449F5, Germany), electron paramagnetic resonance spectroscopy (EPR, Bruker A300, Germany), X-ray photoelectron spectroscopy (XPS; Thermo Scientific K-Alpha, USA), inductively coupled plasma atomic emission spectrometry (ICP-OES; Agilent 720ES (OES), USA) and ultraviolet-visible spectroscopy (UV-Vis; Agilent Technologies Cary 60 UV-Vis, USA). The powder X-ray diffraction (PXRD) data were collected on the Bruker D8 Advance diffractometer using a Cu target radiation with a wavelength of 1.5406 Å, a step size of 0.01, a scanning speed of 3 deg/min, and a scanning range of $2\theta = 2\text{-}30^\circ$. The diffraction data were fully fitted using the Pawley refinement method, and the refinement was completed using the Materials Studio software. During the refinement process, the basic unit of the unit cell was taken as the starting point, and the space group was fixed as P1. The refinement parameters included zero point shift, background, lattice and pseudo-voigt. Keep fractional coordinates fixed during lattice changes. The refinement results were evaluated using the weighted profile R-factor (R_{wp}) and the profile R-factor (R_p). The electrochemical studies were carried out by electrochemical workstation (CHI760E, Shanghai Chenhua)

2. Synthesis of pillar[5]arenes-based ligand

Pillar[5]arenes-based ligand CHO-P5 was synthesized according to the route in Scheme S1.^[S1]



Scheme S1. The synthesis route of CHO-P5.

Compound **I**: 1,4-dimethoxybenzene (20.73 g, 150.10 mmol) and polyformaldehyde (4.60 g, 150.10 mmol) was dissolved in 500 mL of 1,2-dichloroethane. Next, 75 mL of trifluoroacetic acid (TFA) was added into the solution rapidly and reflux at 80°C for 3 h. After cooling to room temperature, the mixture was quenched by methanol and white precipitate was obtained. Vacuum filtration was carried out, and the filter cake was rinsed with methanol. The crude product was purified by column chromatography using methanol as the eluent. Compound **I** was obtained as a white solid (Yield: 11.41 g, 50.7%). ¹H NMR (400 MHz, CDCl₃) δ: 6.81 (s, 10H), 3.77 (s, 10H), 3.68 (s, 30H).

Compound **II**: Compound **I** (6.00 g, 7.99 mmol) was dissolved in 200 mL of dichloromethane, ammonium cerium nitrate (CAN) (8.76 g, 15.98 mmol) was dissolved in 16 mL of water. Next, the CAN solution was slowly dropped into the system within 25 minutes under rapid stirring. After the addition was completed, the solution was further stirred for 5 minutes. The mixture was quenched by water and then extracted by dichloromethane for three times. The organic phase was washed with saturated salt water, then dried with Na₂SO₄. After filtration, it was concentrated under reduced pressure to obtain the crude product. The crude product was purified by column chromatography using dichloromethane/petroleum ether 1:1 (v/v) as eluent. Compound **II** was obtained as a red solid (Yield: 3.86 g, 67%). ¹H NMR (400 MHz, CDCl₃) δ: 6.84 (s,

2H), 6.81 (d, $J = 4.1$ Hz, 4H), 6.67 (s, 4H), 3.79 (d, $J = 3.1$ Hz, 6H), 3.75 (s, 6H), 3.72 (d, $J = 2.0$ Hz, 12H), 3.64 (s, 6H), 3.59 (s, 4H).

Compound III: Compound **II** (1.80 g, 2.48 mmol) was dissolved in 74.66 mL of tetrahydrofuran, and then 32 mL of NaBH₄ (0.48 g, 12.69 mmol) aqueous solution was added. After 30 minutes of reaction, the solution rapidly lightened from red and finally turned light yellow. The mixture was quenched by HCl. After removing tetrahydrofuran under reduced pressure, the aqueous phase was extracted three times with dichloromethane. The organic phase was combined, and washed with saturated salt water. The organic phase was dried with Na₂SO₄, filtered and concentrated under reduced pressure to obtain the crude product. No purification was required and the next step can be carried out directly.

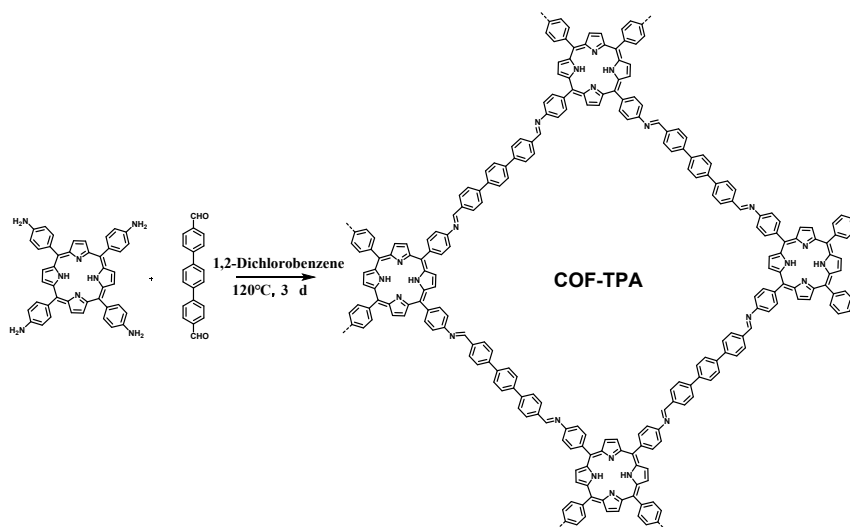
Compound IV: The crude product of compound **III** (1.80 g, 2.49 mmol) was dissolved in 90 mL of dichloromethane. Then, 3 mL pyridine was added. Next, trifluoromethanesulfonic anhydride (7.12 mL, 42.33 mmol) was dropped in an ice bath. The reaction was carried out at room temperature for 24 h. The mixture was quenched by ice water. The aqueous phase was extracted three times with dichloromethane. The organic phase was combined, and washed with saturated salt water. The organic phase was dried with Na₂SO₄, filtered and concentrated under reduced pressure to obtain the crude product. The crude product was purified by column chromatography using dichloromethane/petroleum ether 1:2 (v/v) as eluent. Compound **IV** was obtained as a white solid (Yield: 3.35 g, 64.3%). ¹H NMR (400 MHz, CDCl₃) δ : 7.33 (s, 2H), 6.80 (s, 2H), 6.78 (s, 2H), 6.76 (s, 2H), 6.70 (s, 2H), 3.85 (s, 4H), 3.79 (s, 6H), 3.73 (s, 6H), 3.69 (s, 6H), 3.66 (s, 6H), 3.61 (s, 6H).

CHO-P5: Compound **IV** (2.00 g, 2.03 mmol) and *p*-aldehyde phenylboric acid (1.52 g, 10.13 mmol) were dissolved in 80 mL of tetrahydrofuran, and 20 mL of K₂CO₃ (3.36 g, 24.32 mmol) aqueous solution was added. Next, Pd(PPh₃)₄ (374.68 mg, 324.23 mmol) was added under N₂ atmosphere and refluxed at 80°C for 72 h. After the reaction was completed, after cooling to room temperature and evaporating under reduced pressure to remove the solvent tetrahydrofuran, the crude product was extracted three times with dichloromethane, and the organic phases were combined. The organic phase

was dried with Na₂SO₄, filtered and concentrated under reduced pressure to obtain the crude product. The crude product was purified by column chromatography using dichloromethane/petroleum ether 1:1 (v/v) as eluent as the eluent. Compound **IV** was obtained as a white solid (Yield: 1.28 g, 70%). ¹H NMR (400 MHz, CDCl₃) δ : 10.02 (s, 2H), 7.63 (d, *J* = 7.7 Hz, 4H), 7.08 (d, *J* = 7.6 Hz, 4H), 6.86 (s, 2H), 6.73 (d, *J* = 15.5 Hz, 4H), 6.55 (s, 2H), 5.92 (s, 2H), 3.94 - 3.83 (m, 4H), 3.82 - 3.71 (m, 6H), 3.68 (s, 6H), 3.57 (s, 6H), 3.38 (s, 6H), 3.30 (s, 6H).

3. Synthesis of pillar[5]arenes-derived COFs

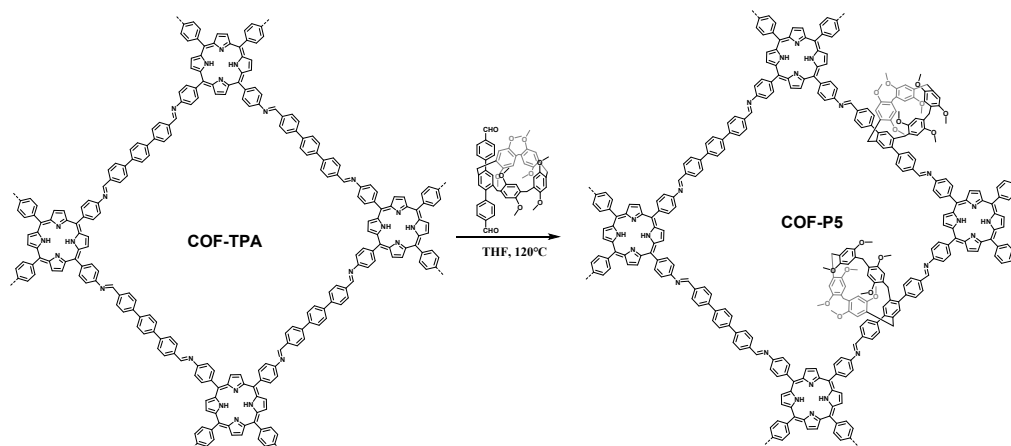
COF-TPA: As shown in Scheme S2, 14.3 mg amino ligands 5,10,15,20-tetrakis(4-aminophenyl)porphyrin (TAPP) and 16.9 mg aldehyde ligand 4,4''-p-terphenyldicarboxaldehyde (TPA) was added to a Schlenk tube. Next, 1 mL 1,2-dichlorobenzene was added into the solution. The mixed solution was ultrasonically dispersed for 15 min and 0.1 mL of CH₃COOH (6.0 mol/L) was added into the solution, then carried out freeze-pump-thaw process for three times. Finally, the mixture was stayed at 120°C for 3 days. The obtained crude product was washed with methanol and collected by filtering. After vacuum drying at 60°C, a brown solid namely COF-TPA (Yield: 78%) was finally collected.



Scheme S2. The synthesis route of COF-TPA.

COF-P5: As shown in Scheme S3, COF-TPA (20 mg) and CHO-P5 (108 mg) was added to a Schlenk tube. Next, super-dry tetrahydrofuran was added into the solution. The mixed solution was ultrasonically dispersed for 15 min and 0.4 mL of CH₃COOH

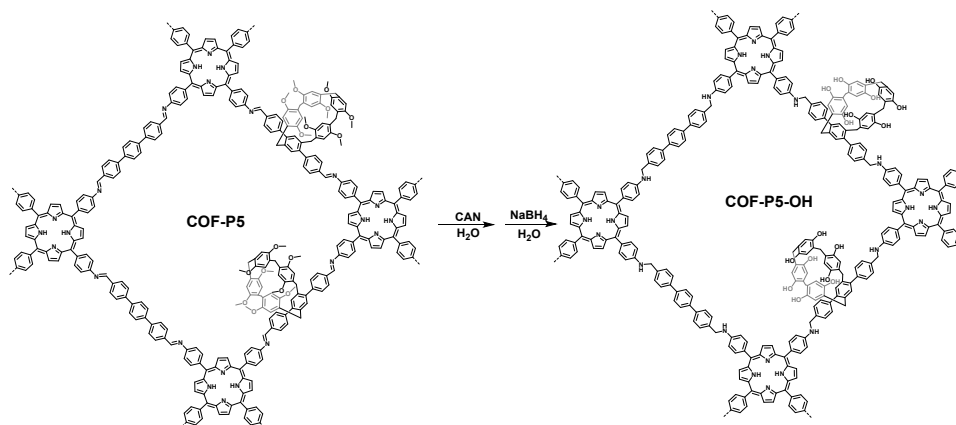
(6.0 mol/L) was added into the solution, then carried out freeze-pump-thaw process for three times. Finally, the mixture was stayed at 120°C for 3 days. The obtained crude product was washed with methanol and tetrahydrofuran for three times, respectively. After vacuum drying at 60°C, the product namely COF-P5 (25 mg) was finally collected.



Scheme S3. The synthesis route of COF-P5.

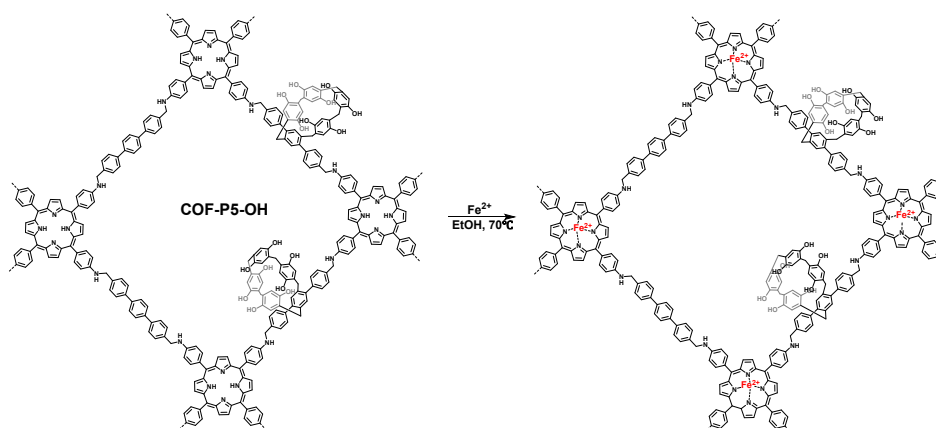
COF-P5-OH: As shown in Scheme 4, COF-P5 (20 mg) and 10 mL of deionized water were added into a single-necked flask. The solution was ultrasonically dispersed for 15 min and 5 mL of CAN solution (62 mg) was added into the solution and stirred at room temperature for 30 minutes. After the reaction was completed, it was washed twice with water and twice with ethanol, and then vacuum-dried to obtain blackish-brown powder named COF-P5=O (19 mg).

COF-P5=O (20 mg) and 10 mL of deionized water were added in a single-necked flask, and ultrasonically dispersed for 15 minutes. Next, 5 mL of NaBH₄ aqueous (8 mg) was added into the solution, and stirred at room temperature for 30 minutes. After the reaction was completed, the mixture was washed three times with water and ethanol respectively, and then vacuum dried to obtain blackish-brown powder named COF-P5-OH (18 mg).



Scheme S4. The synthesis route of COF-P5-OH.

COF-P5-OH-Fe: As shown in Scheme 5, COF-P5-OH (30 mg) and 20 mL of ethanol were added into a 48 mL pressure-resistant bottle. The solution was ultrasonically dispersed for 15 minutes, and blow with N₂ for 15 minutes. Next, FeCl₂·4H₂O (8.6 mg) was added into the mixture and ultrasonically for 10 minutes and reacted at 70°C for 4 hours. After the reaction was completed, the precipitate was collected and washed three times with ethanol to obtain the brown solid COF-P5-OH-Fe (23 mg, Yield: 75%). COF-TAP-Fe and COF-P5-Fe were prepared in similar method.



Scheme S5. The synthesis route of COF-P5-OH-Fe.

4. Electrochemical studies

The electrochemical impedance spectroscopy was carried out at a frequency range of 10-100 kHz. The electrolyte was [Fe(CN)₆]^{3-/4-} (5 mmol/L) and KCl (0.1 mol/L). The samples of COFs were dispersed by ultrasonic and the uniformly dripped on a fluorine doped tin oxide (FTO) electrode. Mott-Schottky curves were measured at a frequency of 1000, 1500 and 2000 Hz, respectively. The electrolyte was the aqueous solution of

Na_2SO_4 (0.5 M). The working electrodes were prepared as follows: 5 mg of photocatalyst powder was dispersed in the mixture of 475 μL of ethanol and 25 μL of nafion solution (5% w/w, water and isopropyl alcohol), which was dip-coated on the surface of FTO glass substrate and dried. A platinum wire and a saturated calomel electrode were used as the counter electrode and the reference electrode, respectively. The test conditions of i-t curves were the same with Mott-Schottky curves. And the lamp (100 mW/cm^2) was turned on and off for 10 s.

5. OXD-like and POD-like activity measurements

The OXD-like activities of COFs were investigated with the irradiation of white light and without light irradiation, respectively. 30 μL of COFs (0.5 mg/mL), 120 μL of 3,3,5,5-tetramethylbenzidine (TMB, 10 mM) were added into 2850 μL of HAc-NaAc buffer (0.2 M, pH 4.0) and the obtained mixture was incubated at room temperature for 5 min with the irradiation of white light irradiation. It was then transferred to a cuvette for UV-Vis spectroscopy analysis.

The POD-like activities of COFs were investigated with the irradiation of white light and without light irradiation, respectively. 30 μL of COFs (0.5 mg/mL), 120 μL of 3,3,5,5-tetramethylbenzidine (TMB, 10 mM) and 30 μL of H_2O_2 (40 mM) were added into 2820 μL of HAc-NaAc buffer (0.2 M, pH 4.0) and the obtained mixture was incubated at room temperature for 5 min with the irradiation of white light and without light irradiation, respectively. It was then transferred to a cuvette for UV-Vis spectroscopy analysis.

To achieve the optimal analytical performance, pH values of HAc-NaAc buffer solution was optimized. The pH values of the HAc-NaAc buffer solution were changed to 2, 3, 4, 5, 6 and 7, respectively and the above experiment was repeated.

6. Steady-State kinetics test

The steady-state kinetic experiment of COF-P5-OH-Fe was carried out under the optimal conditions with various concentrations of TMB and fixed concentration of H_2O_2 (1.5 mM) or with various concentrations of H_2O_2 and fixed concentration of TMB (1.5 mM), the kinetic tests were operated in time scan mode at 652 nm by microplate reader.

The V_{\max} and K_m were derived via the following equation:

$$1/v = K_m/V_{\max} (1/[S] + 1/K_m)$$

Where v was the initial velocity, V_{\max} was the maximum velocity of reaction, K_m was the constant of Michaelis-Menten equation, and $[S]$ was the concentration of the substrate.

7. Determination of reactive oxygen species (ROS)

To determine the ROS produced by COFs, *p*-benzoquinone (PBQ), histidine (His), catalase (CAT) and tert-butyl alcohol (*t*-BuOH) were selected as the scavenger of $\cdot O_2^-$, 1O_2 , H_2O_2 and $\cdot OH$, respectively. The experimental procedure was as follows: the final concentration of 0.5/1 mM PBQ, CAT, His or *t*-BuOH was added to HAc-NaAc buffer solution (pH 4.0) containing COFs and TMB. Next, the mixed solution was incubated under the irradiation of white light for 5 min, and the absorbance at 652 nm was monitored via a UV-Vis spectrophotometer.

To further verify the species of ROS generated by COFs, $\cdot O_2^-$, $\cdot OH$ and 1O_2 were determined by EPR spectrometer using 5,5-dimethyl-1-pyrroline-1-oxide (DMPO) and 2,2,6,6-tetramethyl-piperidin (TEMP) as spin trapping agents.

8. Antibacterial experiments

The antibacterial effect of COFs was carried out by plate coating method. Single colonies of *Escherichia coli* (*E. coli*) cultured on plates were selected and dissolved in Luria-Bertani (LB) liquid medium, and incubated in an incubator at 37°C for continuous shock culture overnight. The bacteria were re-inoculated in LB medium at 37°C and 200 rpm until logarithmic growth. For plate coating tests, the concentration of bacterial solution was adjusted by phosphate buffer to the value of OD_{600} was 0.4. To investigate the antibacterial effect of the light-responsive POD mimics, the diluted bacterial solution was added into different centrifuge tubes respectively: Control, H_2O_2 , COF-P5-OH-Fe, COF-P5-OH-Fe + H_2O_2 . Next, they were incubated at 37°C for 30 min and followed by the irradiation of white light ($100 \text{ mW} \cdot \text{cm}^{-2}$), 850 nm light ($100 \text{ mW} \cdot \text{cm}^{-2}$) or not for 30 min. After incubation, the treated bacterial solution was diluted. And then the diluted bacterial solution was evenly pushed onto the surface of the solid medium and cultured on a plate at 37°C for 14 h. The number of colonies was observed

and counted. What's more, ascorbic acid was added to the above groups as a ROS scavenger to investigate the photocatalytic antibacterial mechanism of COFs. The antibacterial effect of COFs on *Staphylococcus aureus* (*S. aureus*) was carried out by the similar method.

9. Supplementary figures and tables

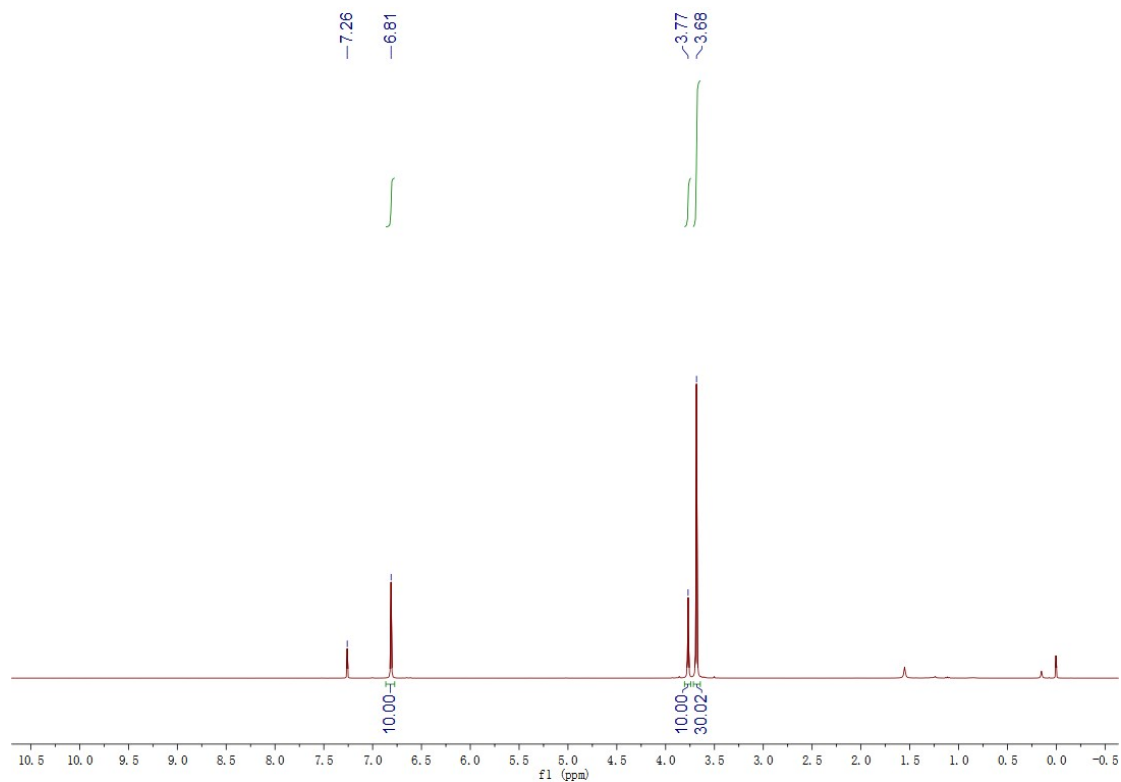


Figure S1. ¹H NMR spectrum of compound I.

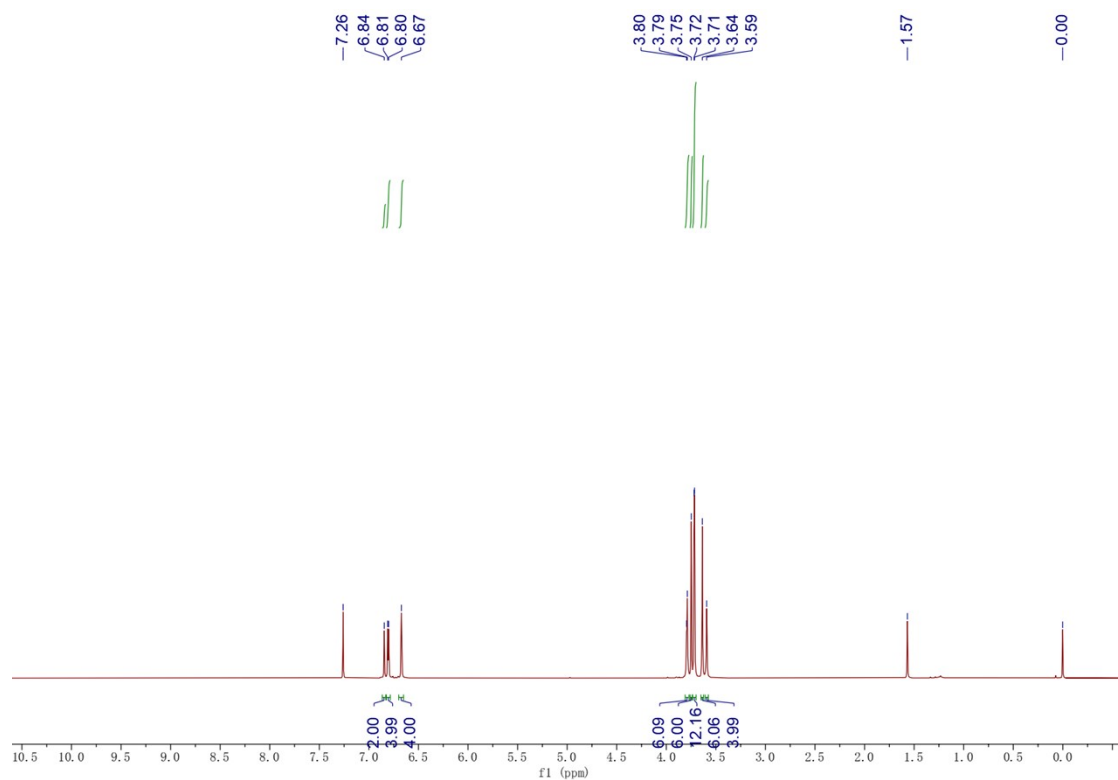


Figure S2. ^1H NMR spectrum of compound **II**.

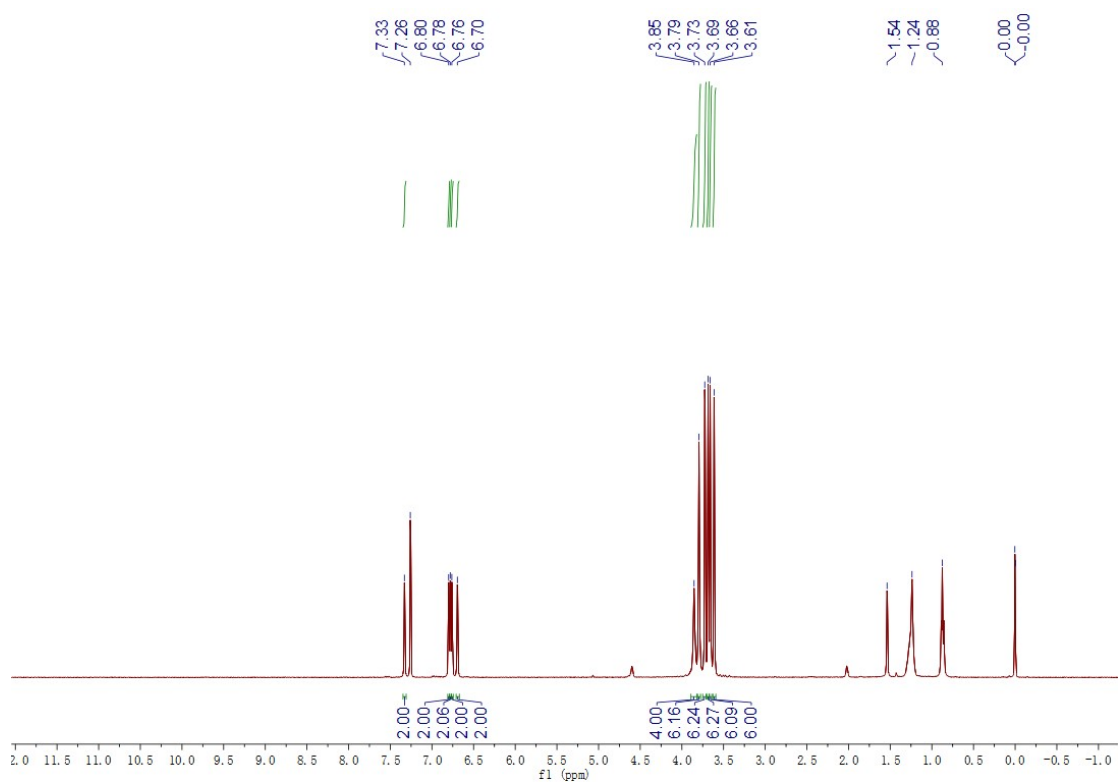


Figure S3. ^1H NMR spectrum of compound **IV**.

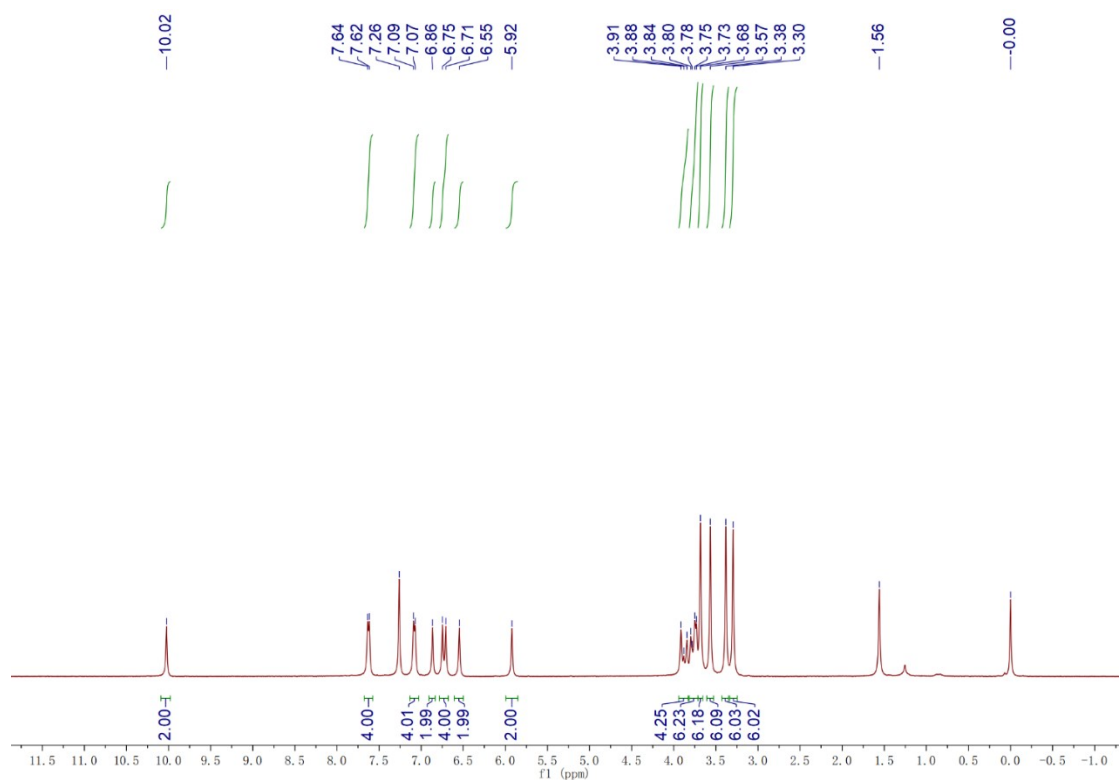


Figure S4. ^1H NMR spectrum of CHO-P5.

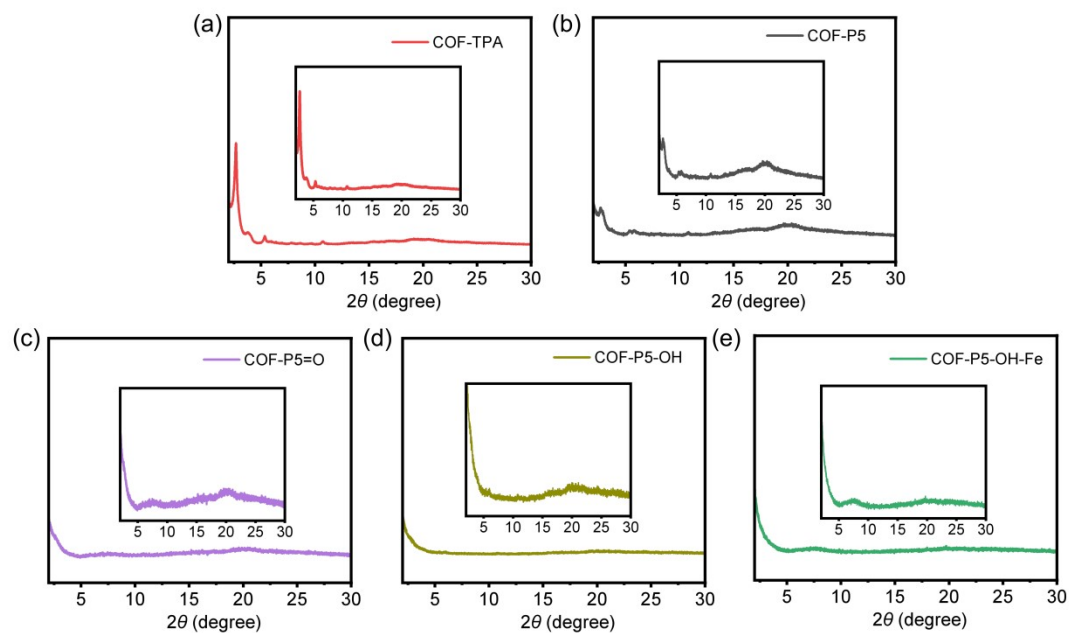


Figure S5. PXRD patterns of (a) COF-TPA, (b) COF-P5, (c) COF-P5=O and (d) COF-P5-OH and (e) COF-P5-OH-Fe.

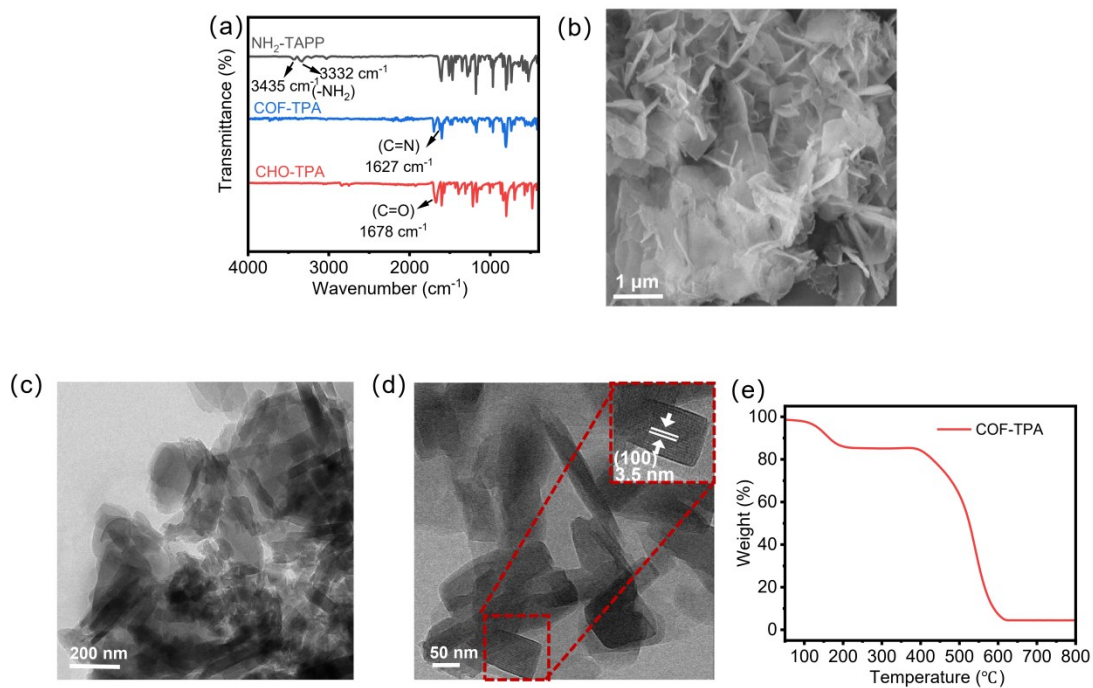


Figure S6. (a) FTIR spectra of COF-TPA; (b) SEM image of COF-TPA; (c) TEM image of COF-TPA; (d) HRTEM image of COF-TPA; (e) TGA of COF-TPA.

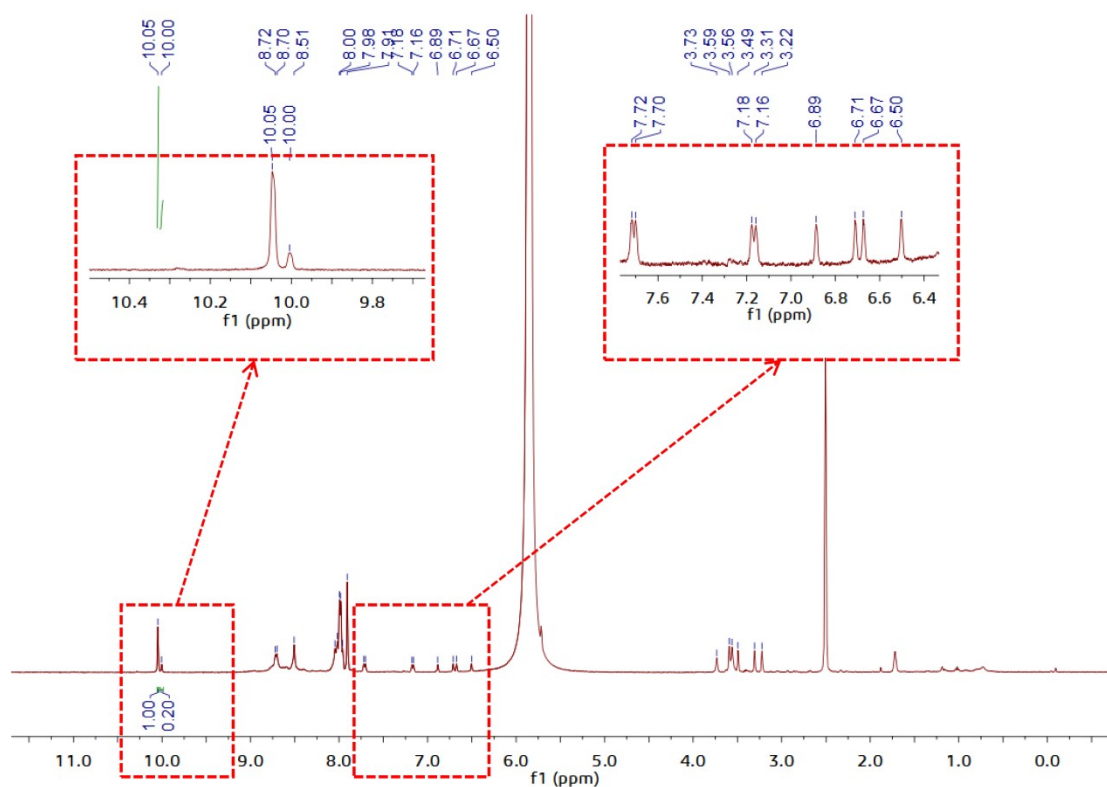


Figure S7. ¹H NMR spectrum of COF-P5.

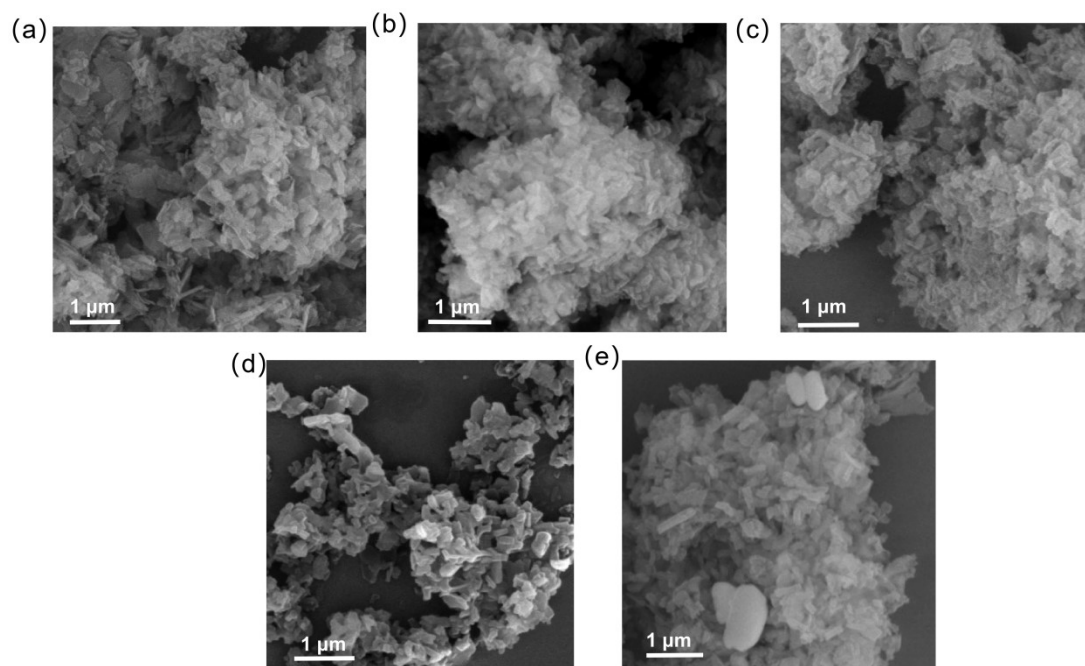


Figure S8. SEM images (a) of COF-P5; (b) COF-P5=O; (c) COF-P5-OH; (d) COF-TPA-Fe and (e) COF-P5-Fe.

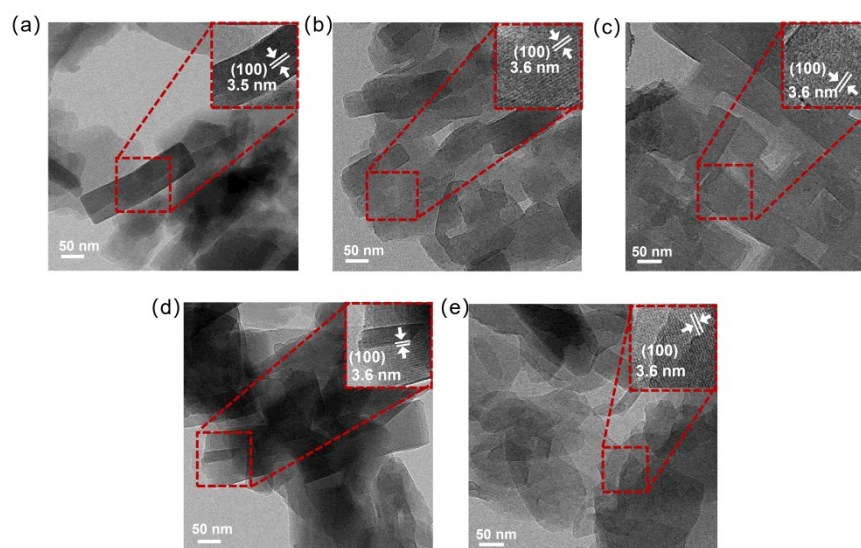


Figure S9. TEM images (a) of COF-P5; (b) COF-P5=O; (c) COF-P5-OH; (d) COF-TPA-Fe and (e) COF-P5-Fe.

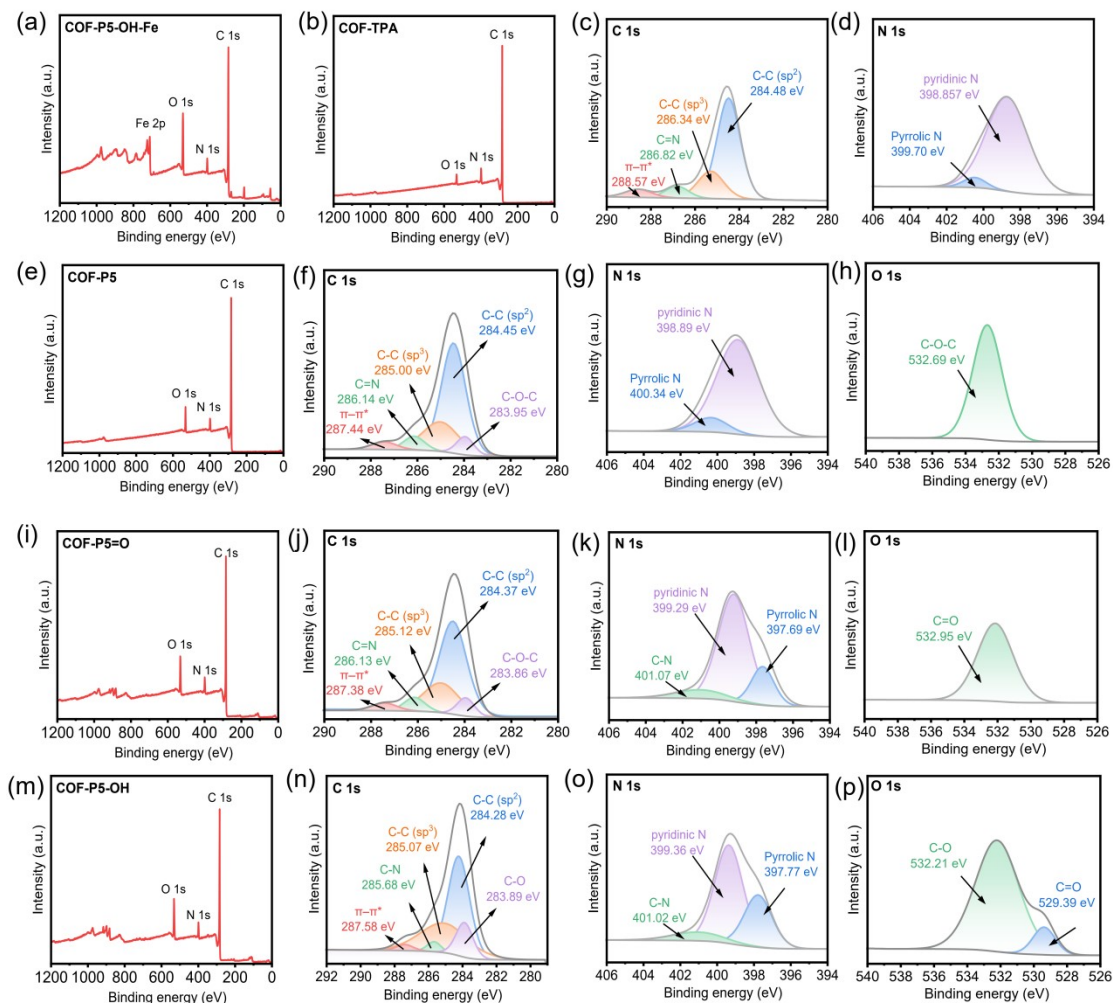


Figure S10. (a) XPS full spectrum of COF-P5-OH-Fe; XPS spectra of COF-TPA: (b) full spectrum, (c) C1s, (d) N1s; XPS spectra of COF-P5: (e) full spectrum, (f) C1s, (g) N1s, (h) O1s; XPS spectra of COF-P5=O: (i) full spectrum, (j) C1s, (k) N1s, (l) O1s; XPS spectra of COF-P5-OH: (m) full spectrum, (n) C1s, (o) N1s, (p) O1s.

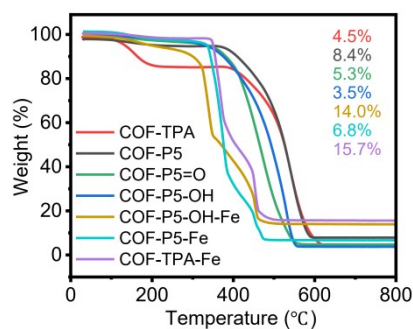


Figure S11. TGA analysis of COF-TPA; COF-P5; COF-P5=O; COF-P5-OH; COF-P5-OH-Fe; COF-P5-Fe and COF-TPA-Fe.

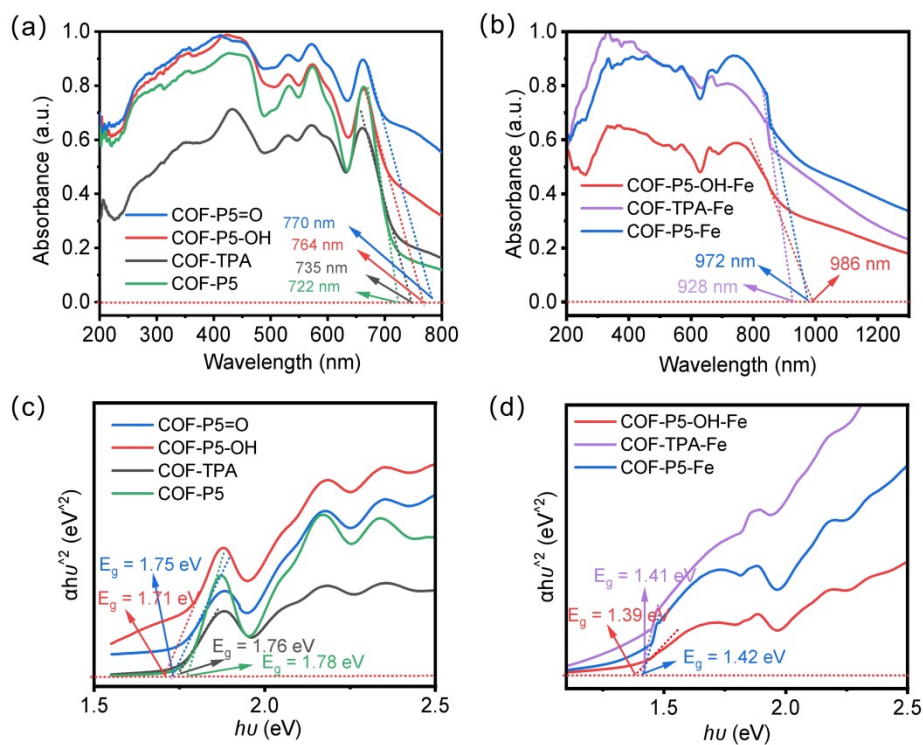


Figure S12. UV-vis DRS spectrum (a and b) and Tauc's band gap plots (c and d).

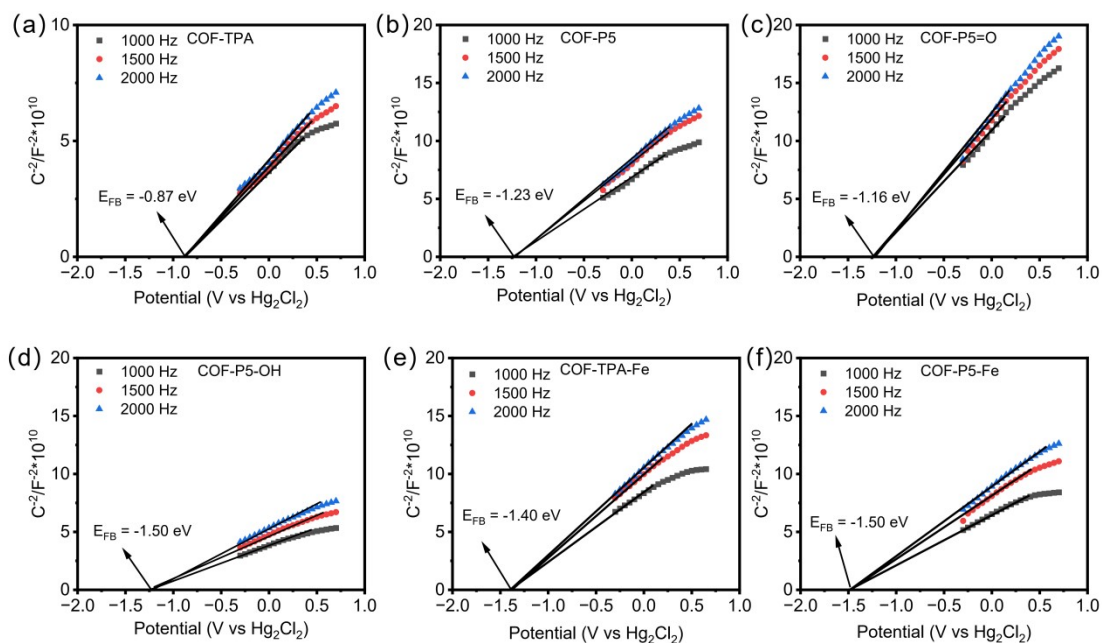


Figure S13. Mott-Schottky plots of (a) COF-TPA; (b) COF-P5; (c) COF-P5=O; (d) COF-P5-OH; (e) COF-TPA-Fe and (f) COF-P5-Fe.

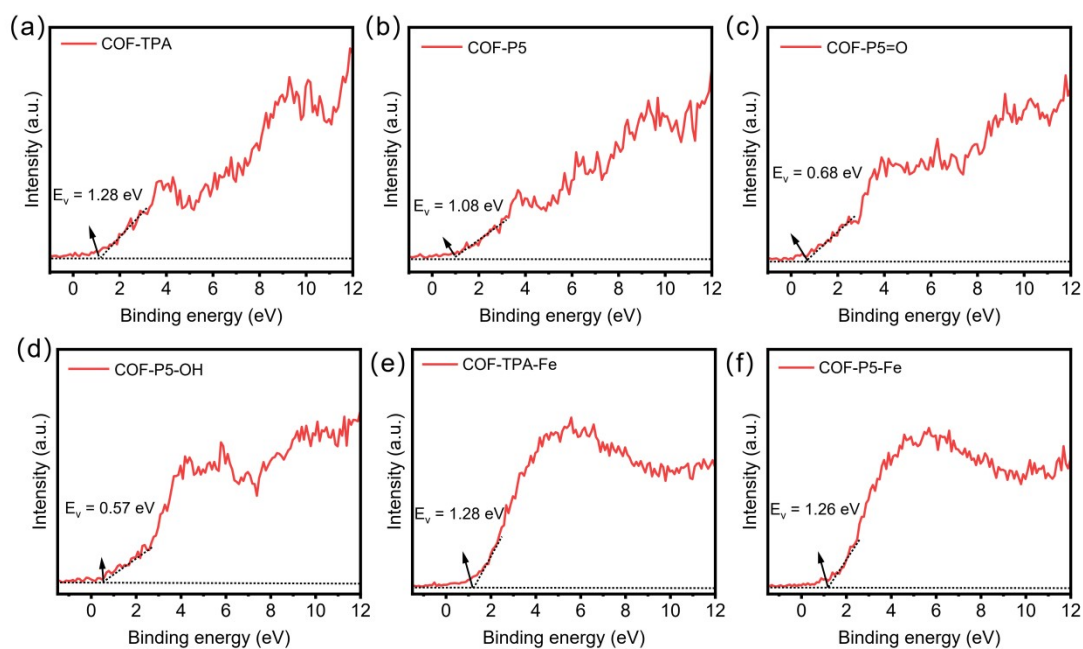


Figure S14. VB-XPS plots of (a) COF-TPA; (b) COF-P5; (c) COF-P5=O; (d) COF-P5-OH; (e) COF-TPA-Fe and (f) COF-P5-Fe.

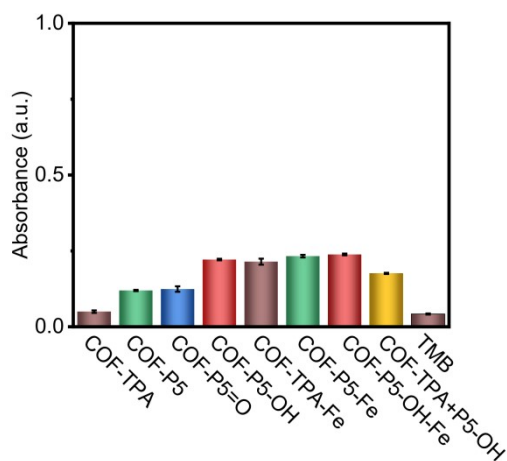


Figure S15. OXD-like activity of different samples under white light irradiation.

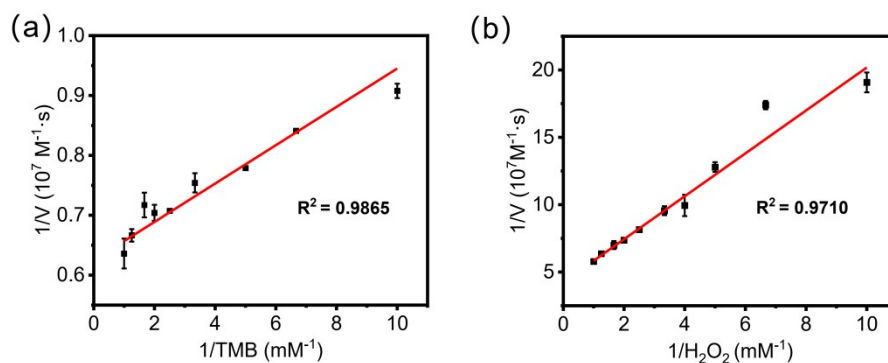


Figure S16. The steady-state kinetic curves of COF-P5-OH-Fe under the irradiation of white light with (a) varying TMB concentration or (b) varying H_2O_2 concentration.

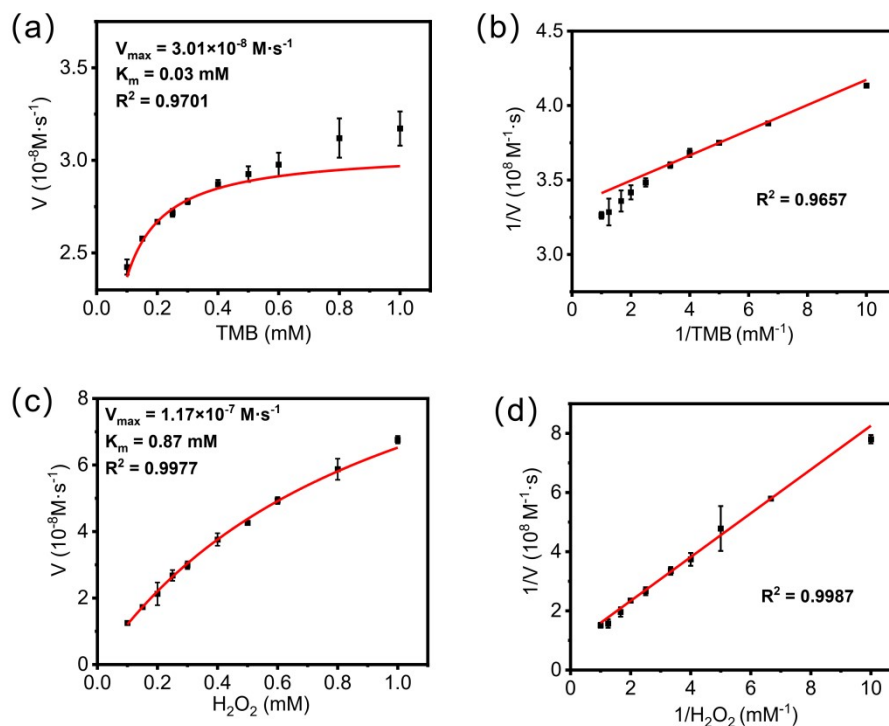


Figure S17. The steady-state kinetic curves and Lineweaver-Burk plots of COF-P5-OH-Fe without light irradiation with (a, b) varying TMB concentration or (c, d) varying H_2O_2 concentration.

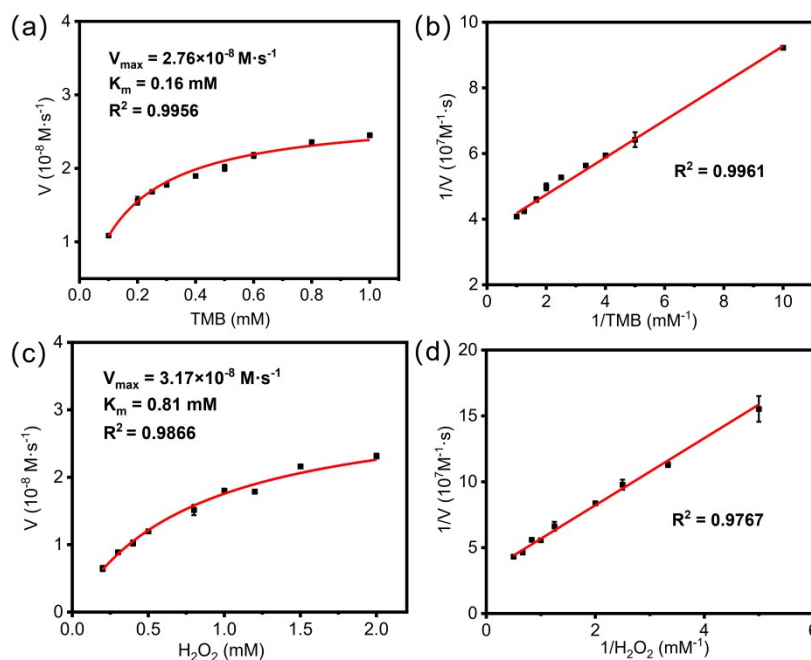


Figure S18. The steady-state kinetic curves and Lineweaver-Burk plots of COF-TPA without light irradiation with (a, b) varying TMB concentration or (c, d) varying H_2O_2 concentration.

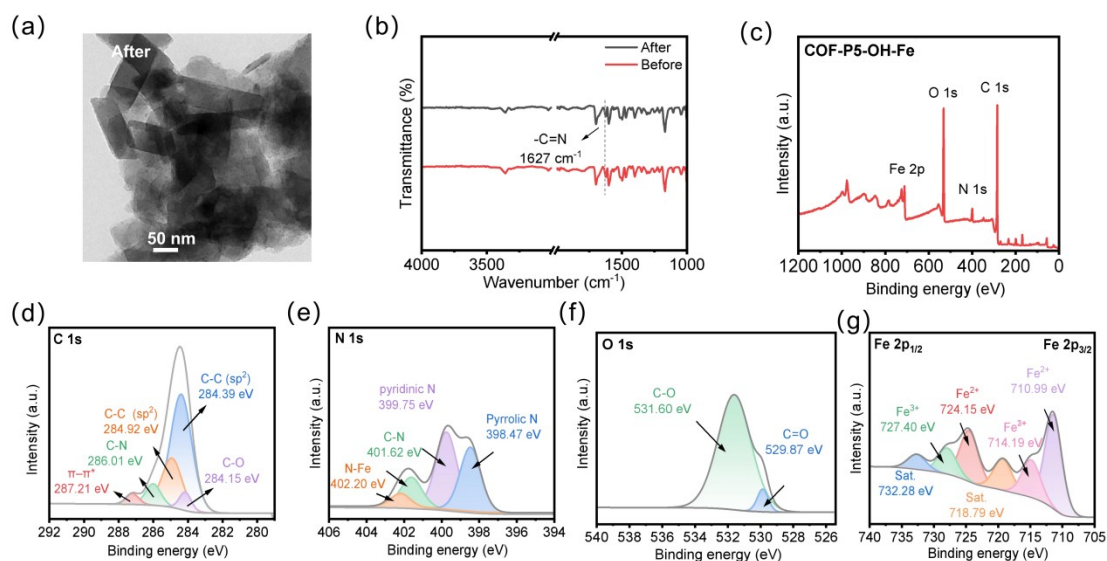


Figure S19. (a) TEM image of COF-P5-OH-Fe after catalysis; (b) FTIR spectra of COF-P5-OH-Fe before and after catalysis; (c-g) XPS spectra of COF-P5-OH-Fe after catalysis.

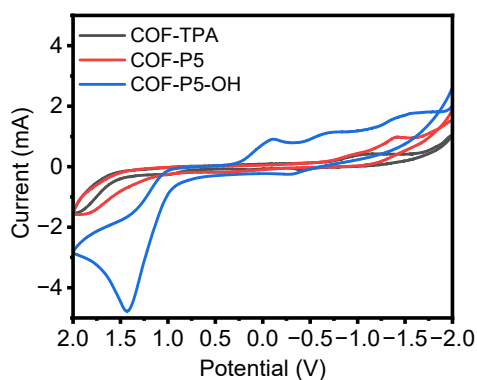


Figure S20. CV curves of different samples.

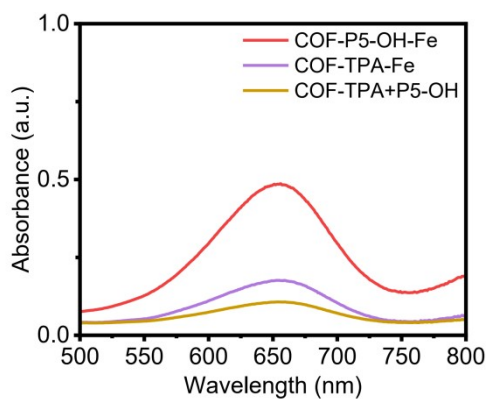


Figure S21. The POD-like activity of COF-P5-OH-Fe and the physical mixture of COF-P5 and COF-TPA-Fe without light irradiation.

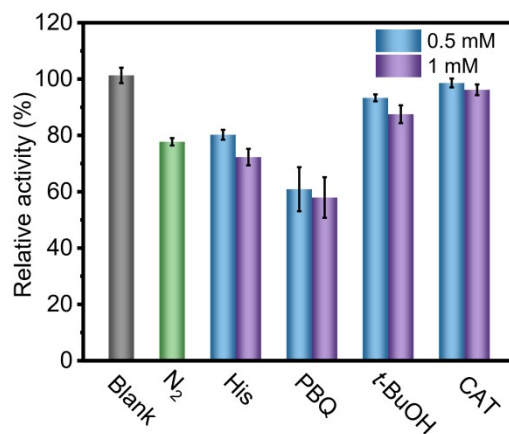


Figure S22. Effects of N₂ and different radical scavengers on the POD-like activity of COF-P5-OH-Fe without light irradiation.

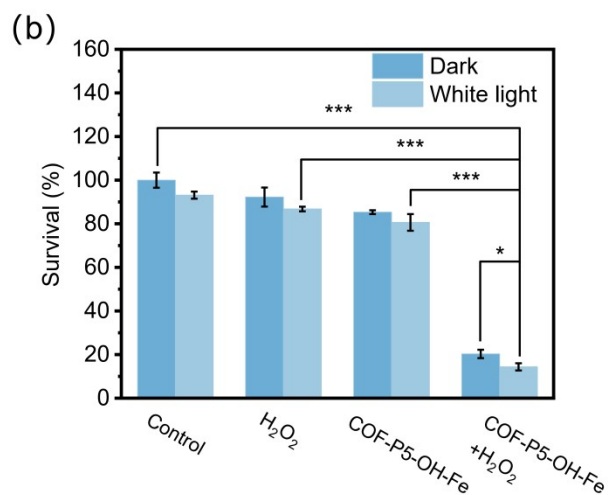
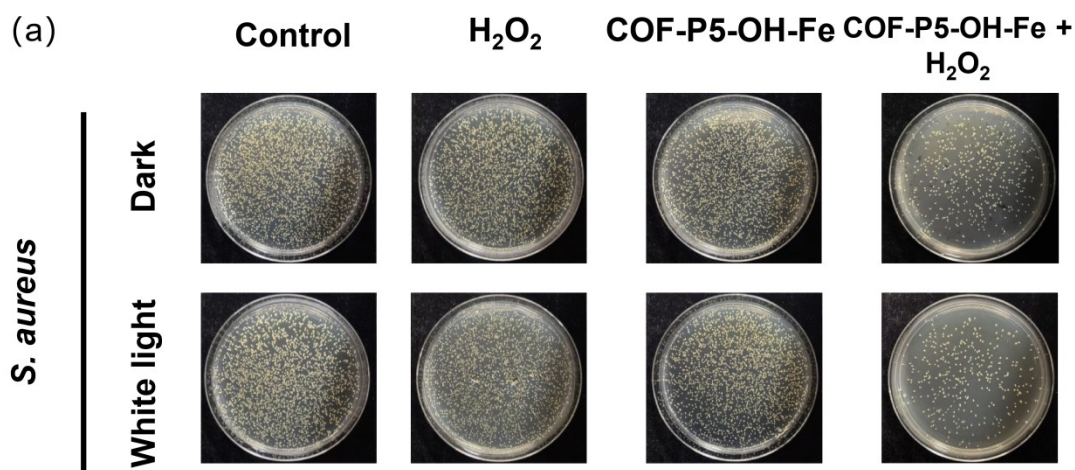


Figure S23. (a) Photographs of *S. aureus* colonies after different treatment; (b) Survival rate of *S. aureus* after different treatments. Data are presented as mean \pm SD ($n = 3$, *** $p < 0.001$, ** $p < 0.01$, * $p < 0.05$).

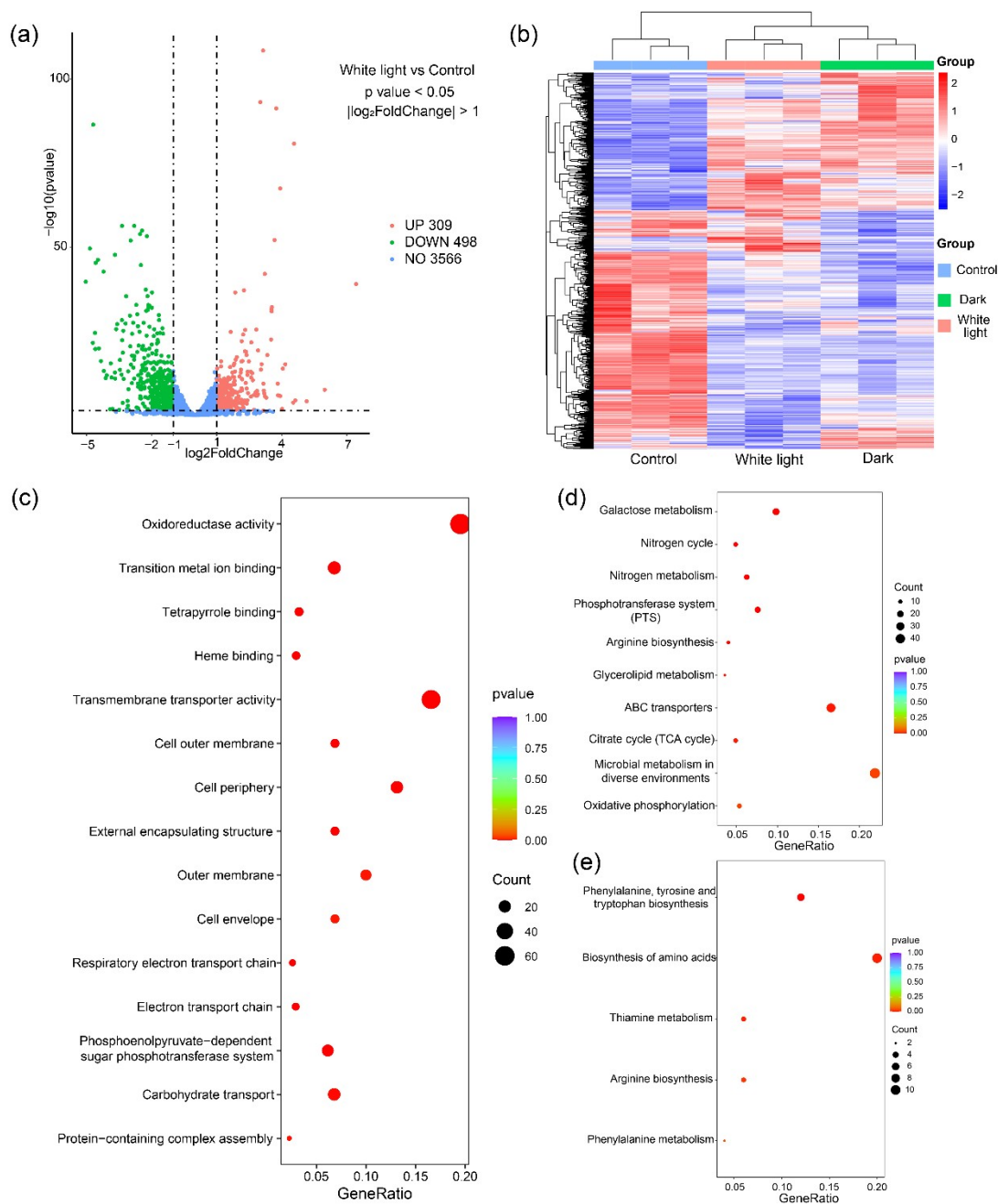


Figure S24. Transcriptomic profiling of *E. coli* treated with the control group and COF-P5-OH-Fe samples: (a) Volcano plots illustrate the differential gene expressions in the white light group and control group; (b) Heat map of differential expressed genes involved in white light group, dark group and control group; (c) GO enrichment analysis for genes that are differentially expressed in the white light group and control group; (d) KEGG pathway enrichment analysis for genes (down regulation) that are differentially expressed in the white light group and control group; (e) KEGG pathway enrichment analysis for genes (down regulation) that are differentially expressed in white light group and dark group, mainly including phenylalanine, tyrosine and tryptophan biosynthesis, biosynthesis of amino acids, thiamine metabolism, arginine biosynthesis, phenylalanine metabolism and etc.

Table S1. Kinetic parameters of different nanozymes.

Catalyst	Substrate	V_{\max} (10^{-8} M \cdot s $^{-1}$)	K_m (mM)	Ref.
HRP	TMB	10.00	0.434	[S2]
	H ₂ O ₂	8.71	3.70	
COF _{Fe/CoP-Ph}	TMB	9.59	0.088	[S3]
	H ₂ O ₂	8.28	2.52	
Citrate-Capped PtNPs	TMB	35	0.055	[S4]
	H ₂ O ₂	32	63	
FePPOP _{EPA}	TMB	4.79	0.091	[S5]
	H ₂ O ₂	2.35	1.95	
PMCS	TMB	10.66	0.224	[S6]
	H ₂ O ₂	12.15	40.16	
MIL-100 (Fe)	TMB	2.10	0.42	[S7]
	H ₂ O ₂	1.40	0.06	
MIL-53 (Fe)	TMB	8.78	1.08	[S8]
	H ₂ O ₂	1.86	0.04	
CF	TMB	68.67	0.21	[S9]
	H ₂ O ₂	28.57	21.02	
Fe ₃ O ₄ @COF@Os (AA)	TMB	134	1.12	[S10]
	H ₂ O ₂	110	1.09	
H ₂ TCPP-NiO	TMB	4.82	0.014	[S11]
	H ₂ O ₂	13.8	39.1	

COF-P5-OH-Fe (White light)	TMB	16.0	0.05	This Work
	H ₂ O ₂	23.5	0.37	
COF-P5-OH-Fe (Dark)	TMB	3.01	0.03	This Work
	H ₂ O ₂	11.7	0.87	

Reflex Pawley Refinement Report

Summary Report

Final R_{wp} :	8.76%	Final R_p :	6.03%
Final R_{wp} (without background):	7.16%	Final CMACS:	0.00%

Setup

2 θ Range (degrees):	2.00-30.00	Step Size (degrees):	0.011
Experiment:	COF-TPA		
Excluded Regions:	-		
Number of Peaks:	1850	Refined:	930

Radiation

Type:	X-ray	Source:	Copper
λ_1 (Å):	1.540562	λ_2 (Å):	1.544390
I_2/I_1 :	0.500	Monochromator:	None
Anom. Dispersion:	No	Polarization:	0.500

Lattice Parameters

Lattice Type:	Triclinic	Space Group:	P 1
---------------	-----------	--------------	-----

Parameter	Value	Refined?
a	35.00903 ± 0.00306	Yes
b	35.01314 ± 0.00471	Yes
c	3.63343 ± 0.00131	Yes
α	90.00000	No
β	90.00000	No
γ	90.00000	No

Pattern Parameters

Profile Function:	Pseudo-Voigt
-------------------	--------------

FWHM

Parameter	Value	Refined?
U	0.40049 ± 0.45626	Yes
V	1.99118 ± 0.08996	Yes
W	-0.04020 ± 0.00180	Yes

Profile

Parameter	Value	Refined?
NA	0.04407 ± 0.00913	Yes
NB	0.02863 ± 0.00083	Yes

Line Shift

Instrument Bragg-Brentano
Geometry:

Parameter	Value	Refined?
Zero Point	0.00000	Yes
Shift #1	0.00000	Yes
Shift #2	0.00000	Yes

Sample Parameters

Crystallite Size

Parameter	Value	Refined?
A	1155.68757 ± 30.76036	Yes
B	152.23017 ± 0.96400	Yes
C	500.00000	No

Lattice Strain

Parameter	Value	Refined?
A	0.00264 ± 0.05691	Yes
B	0.01144 ± 0.08892	Yes
C	0.38234 ± 0.05572	Yes

10. References

- [S1] X. Li, X. Niu, P. Fu, Y. Song, E. Zhang, Y. Dang, J. Yan, G. Feng, S. Lei, W. Hu. Macrocyclic-on-COF photocatalyst constructed by in-situ linker exchange for efficient photocatalytic CO₂ cycloaddition. *Applied Catalysis B: Environment and Energy* 2024, 350, 123943
- [S2] L. Gao, J Zhuang, L Nie, J Zhang, Y Zhang, N Gu, T Wang, J. Feng, D. Yang, Sarah Perrett, X. Yan. Intrinsic peroxidase-like activity of ferromagnetic nanoparticles. *Nature Nanotechnology* 2007, 2(9), 577-583.
- [S3] Y. Bai, W. Gao, J. Wei, B. Yu, L. Zhang, P. Zhu, J. Yu. Biomimetic cascade intelligent paper chip sensor based on bimetallic porphyrin-based covalent organic framework with triple-enzyme mimetic activities. *Chemical Engineering Journal* 2024, 490, 1385-8947.
- [S4] Muhsin Ali, Muhammad Asad Ullah Khalid, Imran Shah, Soo Wan Kim, Young Su Kim, Jong Hwan Lim, Kyung Hyung Choi. A paper based selective and quantitative detection of uric acid using citrate capped Pt nanoparticles (PtNPs) as a colorimetric sensing probe through a simple and remote based device. *New Journal of Chemistry* 2019, 43, 7636-7645.
- [S5] Y. Li, Y. Fang, W. Gao, X. Guo, X. Zhang. Porphyrin-based porous organic polymer as peroxidase mimics for sulfide-ion colorimetric sensing. *ACS Sustainable Chemistry & Engineering* 2020, 10870-10880.
- [S6] B. Xu, H. Wang, W. Wang, L. Gao, S. Li, X. Pan, H. Wang, H. Yang, X. Meng, Q. Wu, L. Zheng, S. Chen, X. Shi, K. Fan, X. Yan, H. Liu. A single-atom nanozyme for wound disinfection applications. *Angewandte Chemie International Edition* 2019, 58(15), 4911-4916.
- [S7] Anil H. Valekar, Bhagwan S. Batule, Moon Il Kim, Kyung-Ho Cho, Do-Young Hong, U-Hwang Lee, Jong-San Chang, Hyun Gyu Park, Young Kyu Hwang. Novel amine-functionalized iron trimesates with enhanced peroxidase-like activity and their applications for the fluorescent assay of choline and acetylcholine. *Biosensors and Bioelectronics* 2018, 100, 161-168.
- [S8] L. Ai, L. Li, C. Zhang, J. Fu, J. Jiang. MIL-53(Fe): a metal-organic framework with intrinsic peroxidase-like catalytic activity for colorimetric biosensing. *Chemistry-A European Journal* 2013, 19(45), 15105-15108.
- [S9] W. Lv, G. Jiang, X. Lin, M. Qian, R. Huang, Z. Li, H. Liu, D. Lin, Y. Wang. An unusual application of multifunctional nanozyme derived from COF: augmenting chemoimmunotherapy while attenuating cardiotoxicity. *Advanced Functional Materials* 2024, 35(2), 2412862.
- [S10] P. Zhou, Y. Dai, X. Lin, Y. Song, Y. Pang, R. Chen, R. Xiao. Specific and magnetic covalent organic framework confined os nanoclusterzyme for interference-free and ultrasensitive biosensing. *Advanced Functional Materials* 2024, 34(34), 2400875.
- [S11] Q. Liu, Y. Yang, H. Li, R. Zhu, Q. Shao, S. Yang, J. Xu. NiO nanoparticles modified with 5,10,15,20-tetrakis(4-carboxyl phenyl)-porphyrin: promising peroxidase mimetics for H₂O₂ and glucose detection. *Biosensors and Bioelectronics* 2015, 64, 147-153.